produced in the non-phase-matchable material and, to a lesser extent, by the sample polycrystallinity. We estimate this DOF to be ≈1 μm. This is in comparison to the 100 nm DOF that is realized in the corresponding one-photon excited experiments, for which the DOF is limited by the penetration depth of the pump beam into the sample.
[30] S. K. Kurtz, T. T. Perry, *J. Appl. Phys.* **1968**, *39*, 3798 – 3813.
[31] TRSHG NSOM experiments using one-photon excitation were not feasible at the time of publication because 3.1 eV photons at the intensities required to observe TRSHG signals caused the SiO_2 NSOM fiber probe to luminesce over a broad spectral range. Two-photon sample excitation, however, did not cause this problem.
[32] C. L. Guo, G. Rodriguez, M. Hoffbauer, A. J. Taylor, *Appl. Phys. Lett.* **2001**, *78*, 3211 – 3213.
[33] R. Braun, B. D. Casson, C. D. Bain, E. W. M. van der Ham, Q. H. F. Vrehen, E. R. Eliel, A. M. Briggs, P. B. Davies, *J. Chem. Phys.* **1999**, *110*, 4634 – 4640.
[34] T. Kawai, D. J. Neivandt, P. B. Davies, *J. Am. Chem. Soc.* **2000**, *122*, 12031 – 12032.
[35] R. C. Dunn, *Chem. Rev.* **1999**, *99*, 2891 – 2927.

Received: July 14, 2003 [Z907]

Low Temperature Conductance Measurements of Self-Assembled Monolayers of 1,4-Phenylene Diisocyanide

Christian J.-F. Dupraz, Udo Beierlein, and Jörg P. Kotthaus*[a]

In the past few years, significant progress has been made in the fabrication and demonstration of molecular wires,[1–3] molecular diodes[4] and switches.[5] Many of these advances have been made possible by using the self-assembly of molecules on nanofabricated semiconductor and/or metallic structures. The most studied molecular system for electronic transport is the Au-SR system, where a self-assembled monolayer (SAM) of an oligomer (R) binds to a gold surface via a thiol group. In order to measure the electrical current through such a molecular layer, a second electrode is needed. This counterelectrode can be provided by an STM tip,[6–9] by another gold wire that can be approached using a mechanical break-junction[1, 10] or by evaporation of a gold layer on top of the SAM.[4] Other techniques employ electromigration of Au[11] or Au particles to achieve small interelectrode distances.[12] In spite of a growing number of publications dealing with electronic transport through molecules, even the conductance and transport mechanisms of relatively simple molecules are not well understood. The reasons lie in the difficulty of providing stable, well-defined metallic contacts at two ends of a molecule, which can allow reproducible transport measurements. It is the purpose of this paper to present two novel sample designs for conductance measurements which were applied to SAMs of the same molecule and to discuss the possible transport mechanisms involved.

One idea for implementing elementary molecular electronic computational functions requires the use of a three-terminal molecular-scale transistor.[13] To this day, only a small number of experiments showing field-effect behavior of molecules have been published.[11, 14, 15] One requirement for a transistor is that it exhibits signal gain which has not been achieved so far in molecular three-terminal devices. Another condition which has to be fulfilled in order to build a molecular field-effect transistors is a strong variation of the density of states (DOS) near the Fermi level of the molecules used. Ideally, the molecules should exhibit a very low conductance at off-resonance conditions and a high transmission in the case that the Fermi level is shifted electrostatically with a gate voltage to resonance. Lang and Avouris[16] have shown theoretically that 1,4-phenylene diisocyanide (PDC), the molecule used in this study, should meet this condition and would therefore be a good candidate for a field-effect device. Temperature-dependent conductance measurements were carried out by Chen et al.[17] with SAMs of PDC, which showed that both hopping and thermal emission of charge carriers could play a role in the conduction mechanisms involved.

Sample Preparation

Two novel fabrication techniques were employed to measure the conductance through a small area of self-assembled molecules.

Method A: Sandwich Architecture

For the first technique, highly p-doped Si with a top layer of 150 nm of SiO_2 was used as a substrate. Metal electrodes were fabricated by a combination of photolithography for the bonding pads and electron beam lithography for the patterning of the fine structures. A first electrode of typically 2 μm length and 200 nm width was defined by electron beam lithography, followed by the evaporation of 3 nm of NiCr and 50 nm of Au. This is followed by a liftoff in acetone and cleaning in ethanol (Figure 1a, I). In the next step, the mask for a second electrode

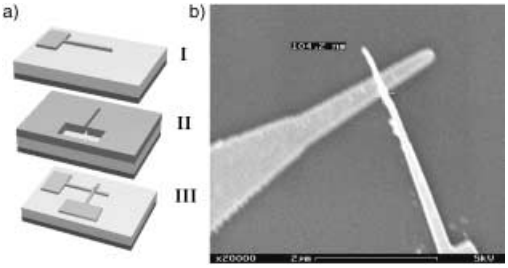

Figure 1. *a) Fabrication of samples of type A and b) SEM image of such a sandwich structure.*

[a] *Prof. Dr. J. P. Kotthaus, C. J.-F. Dupraz, Dr. U. Beierlein*
Center for NanoScience and Sektion Physik
Ludwig-Maximilians-Universität-München
Geschwister-Scholl-Platz 1, 80539 München (Germany)
Fax: (+49) 89 – 2180 – 3182
E-mail: udo.beierlein@physik.uni-muenchen.de

 DOI: 10.1002/cphc.200300706 © 2003 Wiley-VCH Verlag GmbH & Co. KGaA, Weinheim

was patterned perpendicularly to the first electrode in poly(methyl methacrylate) (PMMA) resist (Figure 1 a, II). This created an overlap area of the two electrodes of 50 000 – 100 000 nm^2. After development and rinsing in pure H_2O, the sample was transferred immediately into 1,4-phenylene diisocyanide (1 mM, Aldrich) in hexane. This procedure allowed self-assembly of diisocyanide on those Au surfaces which were not covered by PMMA resist, that is, only the areas between the electrodes. The sample was removed from the solution after 24 – 48 h, rinsed with pure hexane and loaded into a vacuum chamber for evaporation of the second Au electrode (Figure 1 a, III). During the evaporation of 50 nm of Au at a rate of $< 1\ s^{-1}$, the sample was maintained at 77 K. No NiCr adhesion layer was used for the second electrode, since the molecules were intended to be sandwiched between layers of Au. After removal, the chip was bonded to a chip carrier and loaded into an He^4 cryostat. Each chip contained 50 – 200 devices. Some of the devices showed ohmic I-V characteristics with resistances of $< 1\ k\Omega$, which reflects shortened Au – Au junctions. We typically achieved an average yield of 10 % working devices on each chip as judged by the IV traces at 4 K.

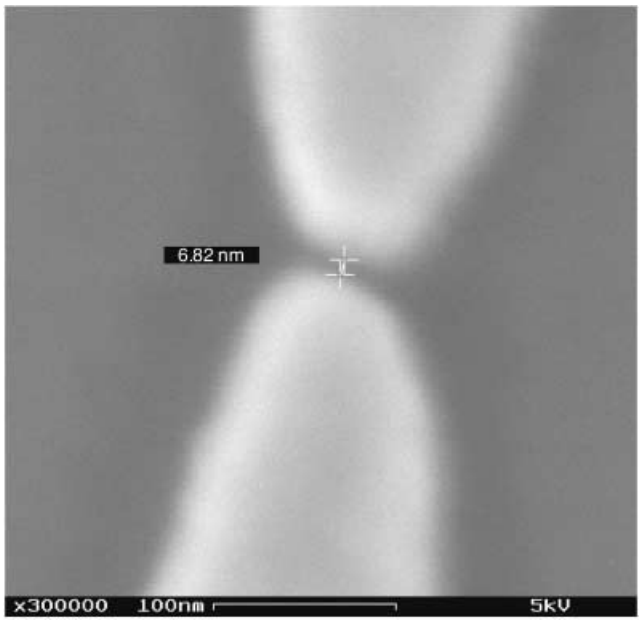

Figure 2. *SEM image of the electrode gap of a multilayer sample (method B).*

Method B: Multilayer Architecture

The second approach to providing contacts on a SAM consisted of fabricating a pair of closely spaced Au electrodes in the chip plane. These electrodes were patterned by standard electron beam lithography on a SiO_2/Si substrate. This was followed by an evaporation of an adhesion layer of 3 nm of NiCr and 50 nm of gold. By carefully optimizing the writing parameters of the LEO982 SEM, electrode distances d of < 10 nm were attained (Figure 2). On each chip, 63 structures were defined with an overall distribution of electrode distances of between 0 and 50 nm. Only devices with $d < 25$ nm were chosen for conductance measurements. The gap between the electrodes was bridged by chains of molecules produced in a sequential process: First, the samples were immersed into a 10 mM solution of 1,4-phenylene diisocyanide in dichloromethane for 60 min and then rinsed in pure dichloromethane. This resulted in a SAM of PDC on both electrodes. Since these molecules have a length of about 1 nm, the electrode gap can not be bridged. In order to allow stacking of several SAMs upon one other, the sample was transferred into a solution of 10 mM cobalt(II)chloride in acetone for 30 min, rinsed in acetone and soaked again in the PDC solution. This leads to an oligomerization of the PDC/Co(II) system by insertion of Co(II) ions between isocyanide end groups of two PDC molecules. This procedure was repeated until the electrode gap was closed by the multilayered structure and a current could be measured by applying a source-drain voltage. Layer-by-layer synthesis of PDC/cobalt(II) films is made possible by the ability of isocyanides to bind to a very wide range of metal centers. This is in turn caused by the formation of stable sigma bonds with high-valent metal centres and π bonds with low-valent metal centers. Ansell et al.[18a, b] and Henderson et al.[18c] characterized such films of PDC/Co(II) by ellipsometry, X-ray photoelectron spectroscopy, attenuated total reflectance-infrared spectroscopy, and reflection – absorption infrared spectroscopy. Their measurements indicate that it is likely that the oligomerization of isocyanides with Co(II) is taking place.

Two-terminal current-voltage characteristics were measured at 4.2 K, 77 K, and at room temperature. Differential dI/dV versus source-drain voltage measurements were carried out using lock-in techniques with a small modulation of the source-drain voltage of a few millivolts at 18 Hz.

Results

Method A

Results showing the variation of conductance (G) with source drain voltage (V_{sd}) were obtained for 32 samples fabricated according to method A. In Figure 3 curves of G versus V_{sd} for three such samples at 4 K are presented.

The results were both reproducible and stable for all low temperature measurements. Each curve comprises a low conductance regime around $V_{sd} = 0$, extending over a voltage range of about 100 – 200 mV. In each curve, the conductance then increases stepwise with increasing voltage. The most prominent features of each curve are the conductance peaks. These peaks are found at different center positions for each device, including devices on the same chip. Some of the peaks for the same device appear to be equidistant in V_{sd} from one another. This is seen most clearly for device 1. Overall the peak distances range between 50 and 200 mV. All curves displayed are asymmetric with respect to $V_{sd} = 0$. So far, this asymmetry could not be related to the fabrication process. Figure 4 shows conductance measurements for device 4 at different temperatures. The conductance peaks measured at 4.2 K are still seen in the measurement at 77 K but are broader and lower in intensity than those of the lower temperature measurement. At room

 © 2003 Wiley-VCH Verlag GmbH & Co. KGaA, Weinheim

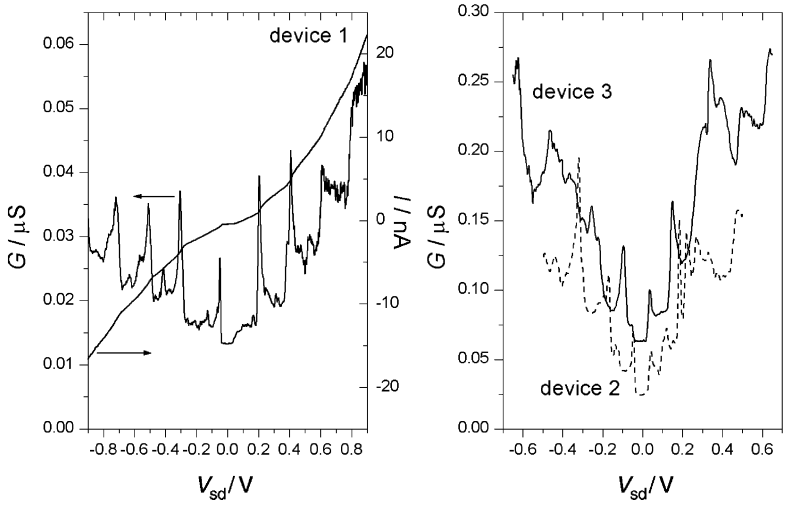

Figure 3. *Conductance versus source-drain voltage curves of devices 1 (overlap area: 72 000 nm^2), 2 (77 000 nm^2) and 3 (65 000 nm^2) at* T = *4.2 K (method A).*

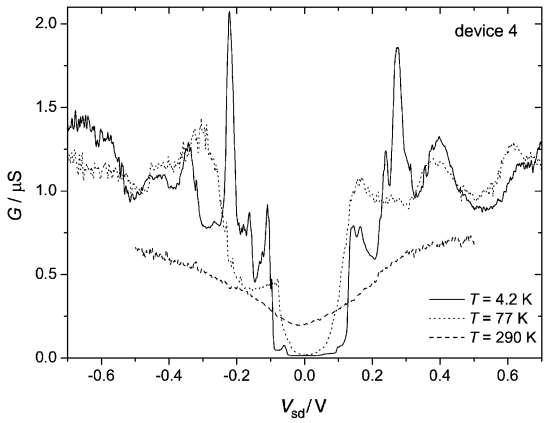

Figure 4. *Source-drain voltage dependence of the conductance of device 4 (overlap area: 65 000 nm^2, method A) at* T = *4.2, 77 and 290 K.*

temperature only a uniform background can be seen with lower conductance than that of the low temperature measurements.

For some of the devices a hysteretic behaviour of the $G(V_{sd})$ curves is observed. As can be seen in Figure 5, most of the peaks

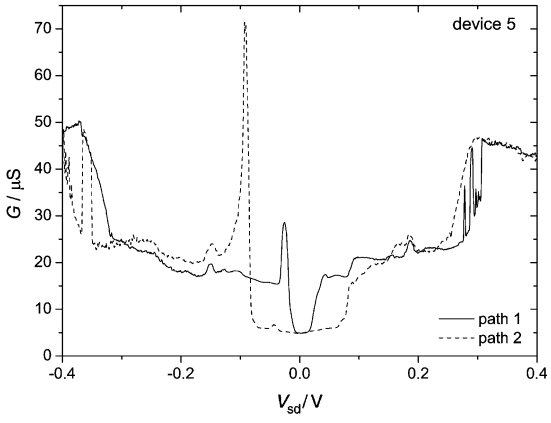

Figure 5. *Hysteresis in the conductance versus source-drain voltage curves for device 5 (T = 4.2 K).*

are shifted between the two curves. It is possible to switch between these two regimes by increasing the source drain voltage above a certain threshold value, for example, for device 5 (Figure 5), the conductance curve corresponding to path 1 can be obtained by driving V_{sd} to values higher than $\approx$0.3 V. The conductance can be switched to that corresponding to path 2 by applying voltages lower than $-$0.3 V. In the voltage range of between +0.3 ($-$0.3) and +0.4 V ($-$0.4 V) two-level fluctuations in the conductance can be observed due to random switching between both regimes. The area of overlap of the two electrodes is proportional to the number of molecules in the SAM and was estimated by scanning electron microscopy (SEM) for each sample. The conductance of the devices is not simply related to the area of overlap and therefore does not depend upon the number of molecules assembled in parallel between the electrodes.

Method B

Conductance and current versus V_{sd} measurements for 27 multilayer samples prepared with method B were carried out. One advantage of this sample architecture is that it allows the recording of current-voltage curves both before and after the self-assembly and oligomerization of the molecules. Figure 6 shows an example of a $I(V_{sd})$ measurement before and after self-assembly of PDC/Co(II) chains at room temperature: The current

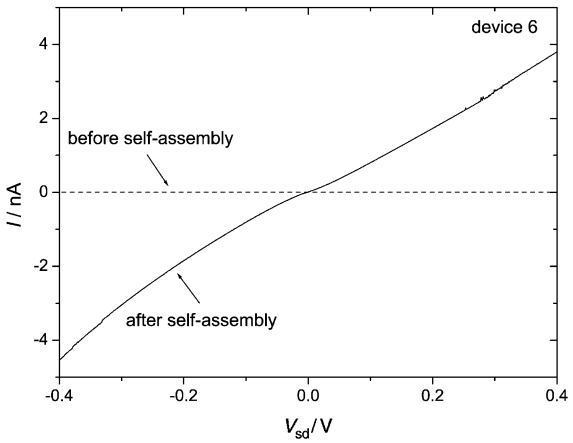

Figure 6. *Current as a function of V_{sd} before and after self-assembly of PDC/Co(II) chains at room temperature.*

between the bare electrodes is practically zero over the whole voltage range. After insertion of the PDC/Co(II) chains, the current increases to 4 nA at V_{sd} = 0.4 V. The gap between the source and drain electrode was d = 15 nm. The conductance measurements for the multilayer samples also show characteristic peak structures. Figure 7 shows $G(V_{sd})$ sweeps for two different samples at 4.2 K. As was the case for the measurements of the

 © 2003 Wiley-VCH Verlag GmbH & Co. KGaA, Weinheim

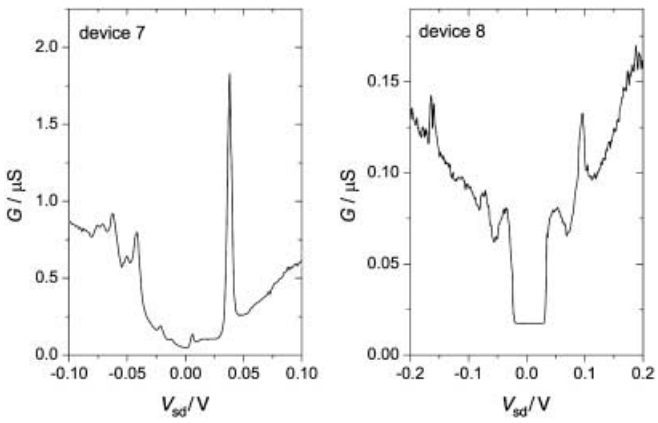

Figure 7. *Conductance versus V_{sd} for two different multilayer device with electrode distances of 9 and 17 nm at $T = 4.2$ K.*

sandwich devices, the position of the conductance peaks and the conductance values differ from sample to sample. A low conductance regime of a width of 50 – 200 mV around zero voltage is observed. All $G(V_{sd})$ and $I(V_{sd})$ curves are asymmetric with respect to voltage inversion. All transport measurements are reproducible and stable at low applied voltage. If V_{sd} is driven to values of higher than approx 2 V, the current drops to very low values, that is, the samples are destroyed. The samples deteriorate after some time if stored in air at room temperature.

Discussion

The conductance traces of the devices gave qualitatively similar results regardless of the measuring technique. This correlation between samples suggests that, in each case, either conductance through a SAM (method A) or a vertical stacking of SAMs (method B) was measured. This is supported by the fact that an ohmic dependence of the current as a function of V_{sd} was detected in the case that the SAM of PDC was absent or in the case that the evaporation of the counterelectrode in the sandwich architecture destroyed the SAM. The fact that it is possible to measure the current for the multilayer technique before and after insertion of the molecules also strongly indicates that our curves correspond to molecular conductance through the PDC/Co(II) chains.

The most intriguing questions surrounding these conductance data are the origins of the conductance peaks and the gap around zero voltage. One possible interpretation is sequential tunnelling of electrons through tunnel barriers formed by the isocyanide groups. At low bias the electrons do not have sufficient energy to tunnel onto the island formed by the phenylene ring, hence the conductivity is low. At higher bias, this Coulomb blockade regime can be overcome. Current flows until the conducting island is charged temporarily with an electron whereby the current becomes blocked again. This corresponds to the appearance of peaks in the $G(V_{SD})$ curves. However, if conduction through individual molecules were being observed, the addition energies would be very high because of the small size of the phenylene ring. Coulomb blockade through single molecules is therefore rather unlikely to occur. If an ensemble of molecules as a whole forms a conducting island, Coulomb charging cannot be excluded. It cannot be ruled out that small Au particles between or near the contacts could also represent such a metallic island. But this would imply that these Au particles have roughly the same size in every device studied, since the peak positions do not vary to a great extent.

A second explanation for the peaks is that these features may reflect coherent transport through the molecular orbitals. In this picture, the Fermi energy at zero bias would be located somewhere between the highest occupied molecular orbital (HOMO) and the lowest unoccupied molecular orbital (LUMO). As the source-drain voltage is increased, the current will increase due to resonant tunnelling when the potential of one of the electrodes is equal to the nearest molecular level. By further increasing the potential difference between source and drain, more and more conductance channels will be opened, which gives rise to a conductance peak for every new molecular level. The DOS calculations for PDC carried out by Lang and Avouris[16] yield an energy difference between Fermi energy and LUMO of 110 meV, which corresponds well to the average width of low conductance regime.

The observed conductance peaks could be understood in terms of the vibrational modes of the molecule. Vibration of molecules would change the coupling between the orbitals of the molecules and the coupling of the molecules to the contacts. If the energy of the incident electron exceeds the vibrational energy, this could lead to variations in the current through the molecules due to energy transfer from the electrons to the molecule. Vibrational modes with energies of 187, 198, 263 and 270 meV were observed in reflection – absorption infrared (RAIR) measurements of PDC self-assembled on silver by Han et al.[19] The modes at 187 and 198 meV are assigned to the phenylene ring modes while the two modes at higher energies are attributed to NC stretching vibrations. Zhitenev et al.[20] report conductance steps periodic in source-drain voltage using self-assembled thiophene oligomers linked to Au contacts via thiol groups. These conductance steps are believed to be caused by a strong electron – vibration coupling which influences the electron's tunnelling probability through the molecules.

The same molecules were used for all of the samples, hence, assuming that the observed phenomena can be attributed to molecular properties alone, the same peak structure in the conductance curves should be observed for every sample. However, this assumption implies that all the molecules couple in the same way to the electrodes. In molecular systems, conductance is highly dependent on the exact position of the linking end group to the surface of the contacts. In samples produced by method A, this surface is probably not atomically flat. Besides, the molecules do not only bind to the upper face of the Au finger, but also on both sides, perpendicularly to the chip surface. This fact may lead to a distribution of different molecule to Au surface positions and to different electrode spacings all over the contact area. Such a distribution is likely to be even more evident for samples prepared by method B. Assuming such a distribution of the coupling to the contacts, no distinct peaks in the conductance curves should show up, since the different

 © 2003 Wiley-VCH Verlag GmbH & Co. KGaA, Weinheim

contributions of all the molecules to the current through the SAM should average out these features. Since there are distinct peaks in the conductance curves of the samples prepared according to both methods, it is reasonable to assume that only some of the molecules in the SAM are active in the electronic transport. These could be those molecules which correspond to the smallest electrode spacing, since the probability of tunnelling varies exponentially with distance. This hypothesis is supported by the fact that the conductance does not scale with the area of the junction in the sandwich architecture.

The conductance in the low voltage regime does not drop to zero for any sample. This probably reflects the imperfection of the SAM, leading to parasitic currents, for example, via direct tunnelling from the source to the drain contact. The asymmetry of the conductance curves which occurs in both methods could be caused by spurious charges, for example, by dangling bonds on the SiO_2 surface. Charge storage in nanoscale devices is known to cause asymmetry. Conductance measurements at higher temperature show that the peak structures disappear only slowly with increasing temperature and can still clearly be seen at 77 K. The temperature dependence of the peak intensity is much stronger for some peaks than for others, which indicates that these features may be caused by different molecules.

In the Coulomb blockade model, the hysteretic behaviour of some of the samples (Figure 5) could be explained by the presence of charge traps between or near the contacts which could be charged and decharged by a high source-drain field. This would induce an additional electric field at neighboring molecules, resulting in a shift of conductance peaks. These defects could possibly be due to PMMA residues, Au particles, or surface states of the substrate. Since the SAM itself is probably not without defects, a contribution to the charge transport due to these defects cannot be ruled out. Molecular rearrangements could also cause hysteresis as proposed by van Ruitenbeek et al.[21]

The multilayer architecture allows a layer-by-layer stacking of SAMs of PDC to form conducting molecular chains. With this technique, chain lengths of up to 30 nm were achieved, bridging gaps between metallic electrodes. Since the number of measured devices is not significant, it is not possible to relate the conductance values with the contact distances which can be measured by SEM.

For both types of devices, no current modulation could be measured when gate voltages of up to 32 V were applied. As expected, the electric field by back gate is strongly screened and cannot penetrate significantly between the source and drain electrodes. This result is supported by numerical simulations. Our results are consistent with results of J.-O. Lee et al.[22]

Conclusion

We have measured the transport properties of self-assembled monolayers of 1,4-phenylene diisocyanide using two novel sample architectures. The conductance of a SAM can either be measured by a vertical Au/SAM/Au stacking (sandwich structure) or by self-assembly of chains of molecules between closely spaced contacts (multilayer structure). We showed that charge transport is possible through self-assembled chains of molecules. This new concept in molecular electronics could lead to the development of larger arrays of molecular devices. The two approaches gave qualitatively similar conductance characteristics. The conductance does not scale simply with the overlap area of the sandwich sample. These findings indicate that only a few molecules contribute significantly to the electronic transport and that the transport properties strongly depend on the local electrode – molecule coupling and the effective electrode spacing. The observed discrete structures in the conductance curves are interpreted as resulting from resonant tunnelling through molecular orbitals or from the excitation of vibrational modes. In this interpretation, the conductance curves contain molecule-specific features as well as unspecific contributions from the coupling to the contacts. It cannot be ruled out that Coulomb blockade plays a role in the conductance of the studied system.

Acknowledgements

We would like to thank F. Simmel for stimulating discussions and A. Kriele, S. Manus, and K. Werhahn for technical support. Financial support by the Sonderforschungsbereich 486 is gratefully acknowledged.

Keywords: electron transport · molecular conductance · monolayers · nanostructures · self-assembly

[1] M. A. Reed, C. Zhou, C. J. Muller, T. P. Burgin, J. M. Tour, *Science* **1997**, *278*, 252.
[2] M. A. Reed, *Proc. IEEE* **1999**, *87*, 652.
[3] S. J. Tans, M. H. Devoret, H. J. Dai, A. Thess, R. E. Smalley, L. J. Geerligs, C. Dekker, *Nature* **1997**, *386*, 474.
[4] C. Zhou, M. R. Deshpande, M. A. Reed, L. Jones, J. M. Tour, *Appl. Phys. Lett.* **1997**, *71*, 611.
[5] J. Chen, M. A. Reed, A. M. Rawlett, J. M. Tour, *Science* **1999**, *286*, 1550.
[6] L. A. Bumm, J. J. Arnold, M. T. Cygan, T. D. Dunbar, T. P. Burgin, L. Jones II, D. L. Allara, J. M. Tour, P. S. Weiss, *Science* **1996**, *271*, 1705.
[7] R. P. Andres, T. Bein, M. Dorogi, S. Feng, J. I. Henderson, C. P. Kubiak, W. Mahoney, R. G. Osifchin, R. Reifenberger, *Science* **1996**, *272*, 1323.
[8] X. D. Cui, A. Primak, X. Zarate, J. Tomfohr, O. F. Sankey, A. L. Moore, T. A. Moore, D. Gust, G. Harris, S. M. Lindsay, *Science* **2001**, *294*, 571.
[9] S. Hong, R. Reifenberger, W. Tian, S. Datta, J. Henderson, C. P. Kubiak, *Superlattices Microstruct.* **2000**, *28*, 289.
[10] J. Reichert, R. Ochs, D. Beckmann, H. B. Weber, M. Mayor, H. v. Löhneysen, *Phys. Rev. Lett.* **2002**, *88*, 176804.
[11] J. Park, A. N. Pasupathy, J. I. Goldsmith, C. Chang, Y. Yaish, J. R. Petta, M. Rinkoski, J. P. Sethna, H. D. Abruña, P. L. McEuen, D. C. Ralph, *Nature* **2002**, *417*, 722.
[12] I. Amlani, A. M. Rawlett, L. A. Nagahara, R. K. Tsui, *Appl. Phys. Lett.* **2002**, *80*, 2761.
[13] A. Aviram, M. A. Ratner, *Chem. Phys. Lett.* **1974**, *29*, 277.
[14] W. Liang, M. P. Shores, M. Bockrath, J. R. Long, H. Park, *Nature* **2002**, *417*, 725.
[15] S. J. Tans, A. R. M. Verschueren, C. Dekker, *Nature* **1998**, *393*, 49.
[16] N. D. Lang, Ph. Avouris, *Phys. Rev. B* **2001**, *64*, 125323.
[17] J. Chen, L. C. Calvet, M. A. Reed, D. W. Carr, D. S. Grubisha, D. W. Bennett, *Chem. Phys. Lett.* **1999**, *313*, 741.
[18] a) M. A. Ansell, E. B. Cogan, C. J. Page, *Langmuir* **2000**, *16*, 1172; b) M. A. Ansell, A. C. Zeppenfeld, K. Yoshimoto, E. B. Cogan, C. J. Page, *Chem. Mater.* **1996**, *8*, 591; c) J. I. Henderson, S. Feng, T. Bein, C. P. Kubiak, *Langmuir* **2000**, *16*, 6183.

 © 2003 Wiley-VCH Verlag GmbH & Co. KGaA, Weinheim

[19] H. S. Han, S. W. Han, S. W. Joo, K. Kim, *Langmuir* **1999**, *15*, 6868.
[20] a) N. B. Zhitenev, H. Meng, Z. Bao, *Phys. Rev. Lett.* **2002**, *88*, 226 801; b) N. B. Zhitenev, A. Erbe, H. Meng, Z. Bao, *Nanotechnology* **2003**, *14*, 254.
[21] J. M. van Ruitenbeek, A. Alvarez, I. Pineyro, C. Grahmann, P. Joyez, M. H. Devoret, D. Esteve, C. Urbina, *Rev. Sci. Instrum.* **1996**, *67*, 108.
[22] J.-O. Lee, G. Lientschnig, F. Wiertz, M. Struijk, R. A. J. Jansen, R. Egberink, D. N. Reinhoudt, P. Hadley, C. Dekker, *Nano Lett.* **2003**, *3*, 113.

Received: February 12, 2003 [Z 706]
Revised: June 17, 2003

Conductance Properties of Stilbenoid Molecules

Rafael Gutiérrez,* Frank Grossmann, and Rüdiger Schmidt[a]

Introduction

In recent years, rapid progress in the field of molecular electronics has been made. Novel experimental approaches allow the investigation of the electronic transport properties of small molecular groups or even single molecules connected to macroscopic or mesoscopic electrodes.[1] Effects such as negative differential resistance (NDR)[2–4] and rectification[5, 6] have been demonstrated. Common to this class of systems is the subtle interplay between electronic and structural properties in determining the electronic transport. This makes the search for molecules that exhibit *controllable* conformational changes highly desirable.[7] Thus, recent experiments on conjugated organic molecules have shown reversible conductance switching which can be related to reorientation of single molecules induced by voltage pulses,[8] to internal structural modifications induced by charge transfer within the molecular complex[9, 10] or to conformational changes due to interactions with the environment,[11, 12] such as, for example, an STM tip.[13]

Stilbene (1,2-diphenylethylene) is a prototypical example of a system with a controllable transition between two stable states. This molecule undergoes a *cis–trans* isomerization around the central ethylenic bond under, for example, the influence of a laser field,[14] which suggests a natural way to realize a switching mechanism. Many experimental and theoretical investigations have been carried out in order to understand the electronic and structural properties of the molecule and the mechanism leading to isomerization as well as its optimal control.[14–18] Less theoretical attention has been paid, however, to the electronic transport properties of the isomers and, especially, to the possibility of identifying them via their fingerprints in the conductance spectrum.

Herein, we investigate electron transport in *cis/trans*-stilbene within a carbon-based molecular device, in which the molecule is covalently bound to two carbon nanotubes (CNT), which act as electrodes, via polyene chains. The possibility to develop a carbon-based nanoelectronics has been investigated theoretically[19] and in recent transport experiments.[10] In the following, we will address three different issues for the proposed carbon-based setup: First, we focus on the differences in the conductance spectra of *cis* and *trans*-stilbene, second we investigate the sensitivity of the electronic transport to the molecule–electrode interface topology, and third, we study modifications of the conductance around the Fermi energy induced by variations in the $(CH)_n$ chain length.

Theoretical Methods

Modern electronic transport calculations for molecular wires started to flourish in the early 1990s, triggered by work of the Ratner[20] and Datta[21] groups. In our computational approach[22] we combine a density-functional-based tight-binding (DF-TB) formalism[23] with numerical Green function techniques to investigate electronic transport within the Landauer theory. The basic quantity to be calculated in the following is the two-terminal conductance $g = (e^2/\pi\hbar)T(E_F)$, which is proportional to the transmission probability $T(E_F)$ at the equilibrium Fermi energy E_F in the linear response regime and at zero temperature. The transmission is calculated using Equation (1):

$$T(E) = 4\mathrm{Tr}[\mathrm{Im}\mathbf{\Sigma}_L(E)\,\mathbf{G}(E)\,\mathrm{Im}\mathbf{\Sigma}_R(E)\,\mathbf{G}^+(E)] \quad (1)$$

The function $\mathbf{G}(E)$, as given by Equation (2), is the Green function of the scattering region including self-energy interactions $\mathbf{\Sigma}_{L,R}$ with the left (L) and right (R) electrodes:[22]

$$\boldsymbol{G}(E) = (E\mathbf{S} - \mathbf{H} - \mathbf{\Sigma}_L - \mathbf{\Sigma}_R)^{-1} \quad (2)$$

The matrices **S** and **H** are molecular overlap and Hamiltonian matrices and the complex self energies are given by Equation (3),

$$\mathbf{\Sigma}_{L,R} = (\mathbf{V}^+_{L,R} - E\mathbf{S}^+_{L,R})\mathbf{g}_{L,R}(E)(\boldsymbol{V}_{L,R} - E\mathbf{S}_{L,R}) \quad (3)$$

where $\mathbf{V}_{L,R}$ and $\mathbf{S}_{L,R}$ are electrode-molecule Hamiltonian and overlap matrices and $\mathbf{g}_{L,R}$ is the Green function of the electrodes. In calculating these quantities in the DF-TB scheme we use a nonorthogonal basis set including the 2s2p carbon valence orbitals and the 1s orbitals of hydrogen. A recent review and further details of the methodology are given in ref. [22].

Additional information on the electronic structure of the different atomic groups can be extracted from the projected density of states (PDOS), obtained from the total DOS of the scattering region by a partial trace, according to Equation (4):

$$\nu_l(E) = -\frac{1}{\pi N_l}\lim_{\eta\to 0^+}\mathrm{Im}\,\mathrm{Tr}_l[\mathbf{G}(E + i\eta)\mathbf{S}] \quad (4)$$

[a] *Dr. R. Gutiérrez, Priv.-Doz. Dr. F. Grossmann, Prof. Dr. R. Schmidt*
Institute for Theoretical Physics
Dresden University of Technology
01062 Dresden (Germany)
Fax: (+49) 351-463-37297
E-mail: gutie@theory.phy.tu-dresden.de

 © 2003 Wiley-VCH Verlag GmbH & Co. KGaA, Weinheim